Inorg. Chem. **1993,** *32,* 6095–6101

Interaction of Metal Ions with Alloxanthine, a Model in Xanthine Oxidase Inhibition by the Drug Allopurinol: Synthesis and Characterization of M(alloxanthine)$_2$(NO$_3$)$_2$·2H$_2$O (M = Cu, Co) and Zn(alloxanthine)$_2$Cl$_2$

Gaby Hänggi, Helmut Schmalle, and Erich Dubler[*]

Institute of Inorganic Chemistry, University of Zürich, Winterthurerstrasse 190,
8057 Zürich, Switzerland

Received January 5, 1993[⊗]

Metal complexes of the xanthine oxidase inhibiting molecule alloxanthine (pyrazolo[3,4-*d*]pyrimidine-2,6-dione) have been synthesized in form of single crystals from aqueous solutions by the reaction of alloxanthine with an excess of the respective metal salts. Crystal data: Cu^{II}(alloxanthine)$_2$(NO$_3$)$_2$·2H$_2$O, $a = 6.985(3)$ Å, $b = 7.582(3)$ Å, $c = 9.051(2)$ Å, $\alpha = 107.50(3)°$, $\beta = 98.49(3)°$, $\gamma = 103.79(3)°$, $V = 429.6(7)$ Å^3, $Z = 1$, space group $P\bar{1}$; Co^{II}(alloxanthine)$_2$(NO$_3$)$_2$·2H$_2$O, $a = 7.408(3)$ Å, $b = 7.838(2)$ Å, $c = 8.666(1)$ Å, $\alpha = 109.72(2)°$, $\beta = 101.35(3)°$, $\gamma = 104.93(2)°$, $V = 434.8(6)$ Å^3, $Z = 1$, space group $P\bar{1}$; Zn^{II}(alloxanthine)$_2$Cl$_2$, $a = 8.267(3)$ Å, $b = 11.256(2)$ Å, $c = 15.804(4)$ Å, $\alpha = \beta = \gamma = 90°$, $V = 1470.6(12)$ Å^3, $Z = 4$, space group *Pbcn*. The structures of all three complexes were refined to final *R* values of 0.030 (Cu), 0.041 (Co), and 0.049 (Zn). In the metal complexes of the type M^{II}(alloxanthine)$_2$(NO$_3$)$_2$·2H$_2$O with M = Cu or Co, the metal ion is situated in the center of a distorted MN$_4$O$_2$ octahedron including two N(9)-coordinating alloxanthine ligands and two water molecules in the equatorial plane and two nitrate groups at the apical positions. A pronounced (4 + 2) elongation of the octahedral geometry is observed in the copper complex. The hydrogen atoms of the neutral, N(9)-coordinating alloxanthine ligand are bonded to the nitrogen atoms N(1), N(3), and N(8). The structure exhibits relatively strong hydrogen-bonding interactions of the types N–H···O and O–H···O. Two pairs of intramolecular bifurcated N–H···O hydrogen-bonding contacts around the hydrogen atoms H(3) and H(8) reveal the formation of indirect chelates, thus stabilizing the molecular complex units. In the monomeric zinc complex Zn(alloxanthine)$_2$Cl$_2$, the metal ion exhibits a tetrahedral coordination by two chloride ions and two alloxanthine ligands monodentately binding through N(9). The hydrogen atoms of the neutral alloxanthine molecule, which are attached at the nitrogen atoms N(1), N(3), and N(8), are involved in hydrogen bonds of the types N–H···O and N–H···Cl. Quantum chemical calculations at the ab initio level predict the 1H,3H,8H-tautomer of alloxanthine to be more stable than the 1H,3H,9H-form by about 13 kJ·mol^{-1}. These findings support those models of the inhibition of xanthine oxidase by alloxanthine, which suggest complexation of the metal center by N(9).

Introduction

The interaction of metal ions with purine derivatives has been the subject of numerous chemical and crystallographic studies, especially in view of the antitumor activity of some metal complexes interacting with cellular DNA.[1] Another important aspect of such investigations is the role of metal ions in mediating the biological functions of nucleic acids.[2,3] In addition, metal ions participate in electron- and hydrogen-transfer processes of many enzymatic reactions involving nucleic acid components.[4] In this context, considerable attention has been devoted in recent years to metal complexes of the oxopurines hypoxanthine and xanthine, being intermediate products of the biological degradation of nucleic acids.

The enzyme xanthine oxidase, containing two molybdenum atoms, two Fe$_4$S$_4$ clusters, and two flavin adenine dinucleotide moieties, catalyzes the biological oxidation of hypoxanthine via xanthine to uric acid, which is subsequently released from the active site of the enzyme.[5] Different disturbances in purine metabolism result in an overproduction of uric acid, thus leading to the deposition of sodium hydrogen urate monohydrate crystals in joints.[6,7] This disease, known as gout, is clinically treated by the antihyperuricemic drug allopurinol (pyrazolo[3,4-*d*]pyrimidin-6-one), which also is a substrate for xanthine oxidase. Alloxanthine (pyrazolo[3,4-*d*]pyrimidine-2,6-dione), the enzymatic oxidation product of allopurinol, inactivates the enzyme by irreversible coordination to the reduced form of the molybdenum center of xanthine oxidase, thus inhibiting uric acid formation.[8,9] Owing to the fact that coordination of the biological substrate molecules is prevented, patients receiving the drug allopurinol excrete much of their purines as hypoxanthine and xanthine. The structural formulas of oxopurines and pyrazolopyrimidines are given in Figure 1.

Kinetic considerations reveal that the inhibition of xanthine oxidase occurs in a two-step reaction. In the first step, a rapid and reversible reaction of the inhibitor molecule with the reduced molybdenum center of the enzyme results in the formation of a Michaelis complex. The following slow and nearly irreversible reaction step involves coordination of the inhibiting molecule to the metal center.[10]

In this context, the coordination chemistry aspects of the antihyperuricemic drug allopurinol and its metabolic oxidation

---

[*] Author to whom correspondence should be addressed.

[⊗] Abstract published in *Advance ACS Abstracts,* November 15, 1993.

(1) Pasini, A.; Zunino, F. *Angew. Chem.* **1987,** *99,* 632.

(2) Kistenmacher, T. J.; Marzilli, L. G. *The Jerusalem Symposia on Quantum Chemistry and Biochemistry*; Jerusalem Academy of Science and Humanities: Jerusalem, 1977; Vol. 9, Part 1, p 7.

(3) Marzilli, L. G.; Kistenmacher, T. J.; Eichhorn, G. L. In *Nucleic Acid-Metal Ions Interactions*; Spiro, T. G., Ed.; Metal Ions in Biology, Vol. I; Wiley: New York, 1980; p 179.

(4) Marzilli, L. G. *Prog. Inorg. Chem.* **1977,** *23,* 255.

(5) Hille, R.; Massey, V. In *Molybdenum Enzymes*; Spiro, T. G., Ed.; Metal Ions in Biology; Vol. 7, Wiley: New York, 1985; p 433.

(6) Elion, G. B. *Angew. Chem.* **1989,** *101,* 893.

(7) Stanbury, J. B., Wyngaarden, J. B., Fredrickson, D. S., Eds. *The Metabolic Basis of Inherited Diseases*; McGraw-Hill: New York, 1987; Vol. 4.

(8) Hille, R.; George, G. N.; Eidsness, M. K.; Cramer, S. P. *Inorg. Chem.* **1989,** *28,* 4018.

(9) Hawkes, T. R.; George, G. N.; Bray, R. C. *Biochem. J.* **1984,** *218,* 961.

(10) Williams, J. W.; Bray, R. C. *Biochem. J.* **1981,** *195,* 753.

0020-1669/93/1332-6095$04.00/0

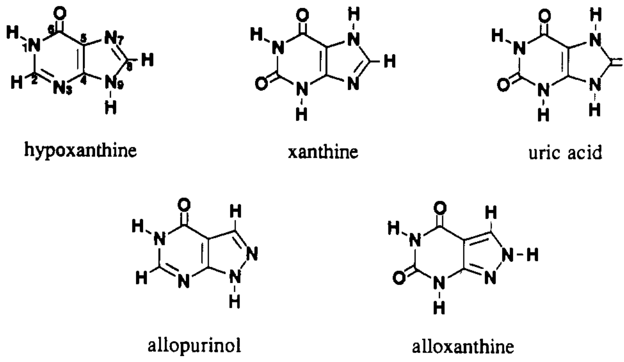

Figure 1. Formulas and numbering scheme of oxopurines and pyrazolopyrimidines.

product alloxanthine are of current interest. No structural information concerning the metal coordination sites of alloxanthine is available so far. As part of our studies on the interactions of metal ions with oxopurines, pyrazolopyrimidines, and thiopurines, the syntheses and structures of the first metal complexes of neutral, unsubstituted alloxanthine are presented in this paper.

Experimental Section

General Procedures. The ligand alloxanthine (pyrazolo[3,4-*d*]pyrimidine-2,6-dione) was prepared according to the method described by Robins,[11] except that precipitation of alloxanthine dissolved in 2 N NaOH was carried out using 2 N H_2SO_4 instead of acetic acid. The metal salts, being of analytical reagent grade, were obtained from Fluka, Buchs, Switzerland. Thermogravimetric data for the three alloxanthine complexes were recorded on a Perkin-Elmer TGS-2 thermobalance in flowing oxygen atmosphere with a heating rate of 10 °C·min^{-1}.

Syntheses. (a) Cu(alloxanthine)$_2$(NO$_3$)$_2$·2H$_2$O. The complex was synthesized by adding a solution of 2.5 g (10.4 mmol) of $Cu(NO_3)_2 \cdot 3H_2O$ in 2 mL of water to 25 mg (0.16 mmol) of alloxanthine suspended in 2 mL of water. The reaction mixture was carefully heated until the ligand was completely dissolved. After 1 week of slow evaporation at a temperature of 40 °C, green crystals of distorted prismatic shape were isolated from the blue-green solution.

(b) Co(alloxanthine)$_2$(NO$_3$)$_2$·2H$_2$O. Single crystals of this coordination compound were prepared by heating a solution of 25 mg (0.16 mmol) of alloxanthine and 5.0 g (17.2 mmol) of $Co(NO_3)_2 \cdot 6H_2O$ in 2 mL of water to boiling. The warm solution was filtered to eliminate any unreacted alloxanthine, and the filtrate was kept for crystallization at a temperature of 40 °C. Five days later, rose-colored crystals with distorted prismatic shape were formed.

The copper and cobalt alloxanthine complexes exhibit strikingly similar thermal decomposition behaviors, indicating their isostructural relationship. Both compounds are thermally stable up to temperature of 170 °C.

(c) Zn(alloxanthine)$_2$Cl$_2$. A 5.2-g (38.2-mmol) sample of $ZnCl_2$ was added to a cold suspension of 50 mg (0.33 mmol) of alloxanthine in 5 mL of water. The cloudy mixture was heated with continuous stirring until complete dissolution of the ligand was observed. The solution was filtered, and the filtrate was kept for crystallization at a temperature of 40 °C. Within 5 weeks, the product appeared in the form of very thin transparent distorted hexagonal platelets.

The complex is thermally stable up to 290 °C and is subsequently decomposed to ZnO in a two step reaction without the formation of a stable intermediate.

Analytical data are given in Table I.

Crystallographic Studies. Intensity data were collected at room temperature on an Enraf-Nonius CAD-4 diffractometer with graphite-monochromatized Mo Kα radiation (λ = 0.7107 Å) using the ω–2θ scan technique with variable scan speeds. During data collection, three standard reflections were monitored at an interval of every 3 h to check crystal stability. For the copper complex, a decrease of the intensities of 1.1% was observed, and for the cobalt complex, a decrease of 2.0% was observed, whereas for the zinc complex no loss of intensities was noted. The data were corrected for Lorentz and polarization effects, and numerical absorption corrections based on eight carefully indexed crystal faces were applied.

Table I. Analytical Data (%) for Alloxanthine Complexes

compound	C(calc) C(obs)	H(calc) H(obs)	N(calc) N(obs)	Cl(calc) Cl(obs)
Cu(alloxanthine)$_2$(NO$_3$)$_2$·2H$_2$O	22.76	2.29	26.54	
$CuC_{10}H_{12}N_{10}O_{12}$	22.87	2.40	26.39	
Co(alloxanthine)$_2$(NO$_3$)$_2$·2H$_2$O	22.96	2.31	26.77	
$CoC_{10}H_{12}N_{10}O_{12}$	23.02	2.40	26.90	
Zn(alloxanthine)$_2$Cl$_2$	27.27	1.83	25.44	16.10
$ZnC_{10}H_8N_8O_4Cl_2$	27.21	1.83	25.28	16.34

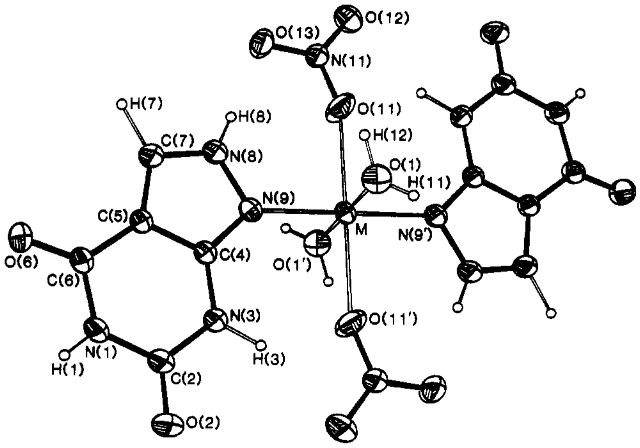

Figure 2. Coordination polyhedron of the metal atom in M(alloxanthine)$_2$(NO$_3$)$_2$·2H$_2$O (M = Cu, Co). The thermal ellipsoids shown refer to the copper complex and are drawn at the 50% probability level.

The structure of the complex Cu(alloxanthine)$_2$(NO$_3$)$_2$·2H$_2$O was solved by Patterson synthesis and refined with full-matrix least-squares and successive difference Fourier calculations using the program MOLEN.[12] On the basis of similar unit cells, the cobalt complex Co(alloxanthine)$_2$(NO$_3$)$_2$·2H$_2$O was considered to be isostructural with the copper complex. Therefore, its structure determination was started with the atomic coordinates of the non-hydrogen atoms of the copper analogue. Anisotropic refinements were carried out by minimizing $\sum w(\|F_o\| - \|F_c\|)^2$ with $w = 1/\sigma^2(F_o) + 0.0016F_o^2)$. All hydrogen atoms could be localized in the difference Fourier maps in both compounds. The four hydrogen atoms of the alloxanthine molecule were refined using the riding model in the copper complex, whereas they were included in the refinement with fixed positional and variable thermal parameters for the cobalt complex. The hydrogen atoms of the water molecule were not refined in both complexes.

The structure of the complex Zn(alloxanthine)$_2$Cl$_2$ was determined by Patterson synthesis with the program SHELXS86[13] and refined by minimizing $\sum w(\|F_o\| - \|F_c\|)^2$, with $w = K/\sigma^2(F_o)$ ($K = 1.6131$), by applying SHELX76.[14] All hydrogen atoms could be localized in the subsequent difference Fourier maps and were refined with variable positional and isotropic temperature parameters. All calculations were performed on a computer of the type HDS AS/XL V60 or on a Micro-Vax 3100.

Crystal parameters, details of data collection, and results of the refinements are summarized in Table II. Atomic parameters and equivalent isotropic thermal parameters are listed in Tables III–V.

Discussion

Molecular Structures. The complexes M(alloxanthine)$_2$(NO$_3$)$_2$·2H$_2$O with M = Cu and Co contain molecular centrosymmetric units (Figure 2). The metal ion exhibits a distorted octahedral coordination of two N(9)-binding alloxanthine ligands and two water molecules lying in the equatorial plane and by two nitrate groups occupying the apical positions. The coordinating octahedra are slightly distorted with bonding angles ranging from 87.23(4) to 92.77(4)° in the copper complex and from 87.34(4)

---

[11] Robins, R. K. *J. Am. Chem. Soc.* **1956**, *78*, 784.

[12] *MOLEN, an Interactive Structure Solution Procedure*; Enraf-Nonius: Delft, The Netherlands, 1990.

[13] Sheldrick, G. M. SHELXS86. In *Crystallographic Computing*; Sheldrick, G. M., Krüger, C., Goddard, R., Eds.; Oxford University Press: Oxford, U.K., 1985; p 175.

[14] Sheldrick, G. M. SHELX76: Program for crystal structure determination. University of Cambridge, England, 1976.

Table II. Crystal Data and Structure Determination Parameters

formula	$CuC_{10}H_{12}H_{10}O_{12}$	$CoC_{10}H_{12}N_{10}O_{12}$	$ZnC_{10}H_8N_8O_4Cl_2$
fw	527.81	523.20	438.67
space group (No.)	$P\bar{1}$ (2)	$P\bar{1}$ (2)	*Pbcn* (60)
a, Å	6.985(3)	7.408(3)	8.267(3)
b, Å	7.582(3)	7.838(2)	11.256(2)
c, Å	9.015(2)	8.666(1)	15.804(4)
α, deg	107.50(3)	109.72(2)	90
β, deg	98.49(3)	101.35(3)	90
γ, deg	103.79(3)	104.93(2)	90
V, $Å^3$	429.6(7)	434.8(6)	1470.6(12)
Z	1	1	4
calcd density, $g \cdot cm^{-3}$	2.04	2.00	1.99
obsd density, $g \cdot cm^{-3}$	2.04	2.00	1.98
color	dark green	pink	white
cryst dimens, mm	0.32 × 0.50 × 0.25	0.37 × 0.22 × 0.35	0.31 × 0.28 × 0.13
abs coeff (Mo Kα), μ, cm^{-1}	13.66	10.76	19.75
transm coeff	0.551–0.935	0.682–0.820	0.582–0.753
data collecn range 2θ, deg	2–80	2–80	2–72
range of *h*/*k*/*l* measd	±12/±13/±16	±13/±14/±15	–13,12/0,18/0,26
scan method	ω–2θ	ω–2θ	ω–2θ
scan speed, $deg \cdot min^{-1}$	1.5–16.5	1.7–16.5	1.8–5.5
max measd time/rfln, s	50	50	40
no. of rflcns measd (including stds)	10 756	10 877	7384
R_{av}/no. of rflcns averaged	0.037/10630	0.013/9119	0.036/6423
no. of unique rflcns	5318	5379	3472
rflcns with $I \geq 3\sigma(I)$	4085	4443	1284
no. of variables	168	155	132
largest shift/esd (non-hydrogen par)	0.001	0.01	0.039
final max/min $\Delta\rho$, e/$Å^3$	0.34/–0.53	0.89/–2.18	0.61/–0.93
R^a	0.030	0.041	0.049
R_w^b	0.046	0.054	0.036

[a] $R = \Sigma||F_o| - |F_c||/\Sigma|F_o|$. [b] $R_w = [\Sigma w(|F_o| - |F_c|)^2/\Sigma w|F_o|^2)]^{1/2}$.

Table III. Positional and Thermal Parameters for $Cu(alloxanthine)_2(NO_3)_2 \cdot 2H_2O$

atom	*x*	*y*	*z*	$U_{eq}{}^a/U_{iso}$, $Å^2$
Cu	0.0000	0.0000	1.0000	0.02315(4)
O(1)	0.2598(1)	–0.0175(1)	1.1019(1)	0.0343(3)
N(11)	0.1355(2)	0.4968(1)	1.2369(1)	0.0274(1)
O(11)	0.1108(2)	0.3385(1)	1.1302(1)	0.0559(3)
O(12)	0.2216(2)	0.6481(1)	1.2196(1)	0.0432(3)
O(13)	0.0713(2)	0.4968(1)	1.3577(1)	0.0443(3)
N(1)	0.3954(1)	0.4695(1)	0.6714(1)	0.0287(1)
C(2)	0.3492(2)	0.5300(1)	0.8180(1)	0.0276(3)
O(2)	0.3915(2)	0.7034(1)	0.8951(1)	0.0400(3)
N(3)	0.2574(2)	0.3901(1)	0.8724(1)	0.0280(1)
C(4)	0.2149(2)	0.1984(1)	0.7830(1)	0.0233(1)
C(5)	0.2692(2)	0.1409(1)	0.6372(1)	0.0253(1)
C(6)	0.3635(2)	0.2816(1)	0.5736(1)	0.0275(3)
O(6)	0.4114(2)	0.2460(1)	0.4443(1)	0.0401(3)
C(7)	0.2053(2)	–0.0591(1)	0.5827(1)	0.0299(3)
N(8)	0.1196(2)	–0.1097(1)	0.6911(1)	0.0298(3)
N(9)	0.1219(1)	0.0463(1)	0.8181(1)	0.0271(1)
H(1)	0.440(3)	0.552(2)	0.640(2)	0.041(5)
H(3)	0.236(3)	0.445(3)	0.984(2)	0.049(5)
H(7)	0.236(5)	–0.184(5)	0.486(5)	0.139(13)
H(8)	0.065(3)	–0.229(3)	0.679(3)	0.058(6)
H(11)	0.299	–0.119	1.050	0.076
H(12)	0.289	0.030	1.199	0.077

[a] $U_{eq} = {}^1/_3\Sigma_i\Sigma_jU_{ij}a^*_ia^*_j\mathbf{a}_i \cdot \mathbf{a}_j$.

Table IV. Positional and Thermal Parameters for $Co(alloxanthine)_2(NO_3)_2 \cdot 2H_2O$

atom	*x*	*y*	*z*	$U_{eq}{}^a/U_{iso}$, $Å^2$
Co	0.000	0.000	1.000	0.02050(4)
O(1)	0.2391(1)	–0.0455(1)	1.1121(1)	0.0329(3)
N(11)	0.1291(1)	0.4622(1)	1.2364(1)	0.0234(1)
O(11)	0.1470(1)	0.3033(1)	1.1555(1)	0.0389(3)
O(12)	0.1907(2)	0.5993(1)	1.1979(1)	0.0410(3)
O(13)	0.0572(2)	0.4803(1)	1.3562(1)	0.0405(3)
N(1)	0.3946(1)	0.4673(1)	0.6748(1)	0.0237(1)
C(2)	0.3409(1)	0.5279(1)	0.8229(1)	0.0236(1)
O(2)	0.3730(1)	0.6992(1)	0.9036(1)	0.0350(1)
N(3)	0.2547(1)	0.3875(1)	0.8729(1)	0.0251(1)
C(4)	0.2189(1)	0.1970(1)	0.7760(1)	0.0204(1)
C(5)	0.2779(1)	0.1405(1)	0.6280(1)	0.0214(1)
C(6)	0.3725(1)	0.2814(1)	0.5718(1)	0.0212(1)
O(6)	0.4313(1)	0.2489(1)	0.4445(1)	0.0300(1)
C(7)	0.2176(2)	–0.0599(1)	0.5642(1)	0.0258(1)
N(8)	0.1315(1)	–0.1098(1)	0.6710(1)	0.0262(1)
N(9)	0.1291(1)	0.0446(1)	0.8047(1)	0.0234(1)
H(1)	0.485	0.581	0.674	0.075(8)
H(3)	0.223	0.428	0.977	0.025(4)
H(7)	0.243	–0.154	0.467	0.049(6)
H(8)	0.077	–0.240	0.663	0.047(5)
H(11)	0.297	–0.123	1.059	0.070
H(12)	0.315	0.028	1.207	0.070

[a] $U_{eq} = {}^1/_3\Sigma_i\Sigma_jU_{ij}a^*_ia^*_j\mathbf{a}_i \cdot \mathbf{a}_j$.

to 92.66(4)° in the cobalt analogue. In addition, a pronounced (4 + 2) elongated coordination octahedron is observed in the copper complex. The neutral alloxanthine molecule with the hydrogen atoms attached to the nitrogen atoms N(1), N(3), and N(8) is monodentately coordinating through the remaining pyrazole nitrogen atom N(9). Summaries of bonding distances and angles are given in Tables VI and VII, respectively.

The coordination polyhedron of $Zn(alloxanthine)_2Cl_2$ is illustrated in Figure 3. The zinc ion is lying on a 2-fold symmetry axis and is tetrahedrally surrounded by two chloride ions and by two alloxanthine ligands monodentately coordinating through N(9). The ZnN_2Cl_2 tetrahedron is markedly distorted, as evidenced by the tetrahedron defining angles, varying from 97.8(2) to 121.9(2)°. The plane determined by N(9)–Zn–N(9′) is not perpendicular to the plane defined by N(9′)–Zn–Cl′, the interplanar angle being 85.2°. The neutral 1H,3H,8H-tautomer of alloxanthine again acts as a monodentate ligand, coordinating through the nitrogen atom N(9). Interatomic bond distances and angles are summarized in Tables VIII and IX, respectively.

Hydrogen Bonding and Purine Stacking. Distances and angles assigned to hydrogen-bonding contacts are listed in Table X. In $M(alloxanthine)_2(NO_3)_2 \cdot 2H_2O$ with M = Cu and Co, the hydrogen atoms of the water molecule participate in hydrogen-bonding interactions with the exocyclic oxygen atoms O(2) and O(6) of alloxanthine, thus interconnecting the planes through the coordinating alloxanthine ligands and the nitrate groups via

Table V. Positional and Thermal Parameters for Zn(alloxanthine)$_2$Cl$_2$

atom	*x*	*y*	*z*	$U_{eq}{}^{a}/U_{iso}$, Å^2
Zn	0.0000	0.08012(7)	0.2500	0.0238(2)
Cl	0.2305(1)	−0.0150(1)	0.2321(1)	0.0333(3)
N(1)	0.4450(5)	0.3626(4)	0.4294(3)	0.0230(11)
C(2)	0.4727(6)	0.2635(4)	0.3817(3)	0.0250(13)
O(2)	0.6082(4)	0.2270(4)	0.3653(3)	0.0368(12)
N(3)	0.3389(5)	0.2041(4)	0.3518(3)	0.0249(13)
C(4)	0.1860(6)	0.2467(4)	0.3705(3)	0.0187(11)
C(5)	0.1636(5)	0.3467(5)	0.4204(3)	0.0213(12)
C(6)	0.2979(5)	0.4139(5)	0.4522(3)	0.0232(11)
O(6)	0.2933(3)	0.5041(4)	0.4933(2)	0.0326(9)
C(7)	−0.0049(7)	0.3626(5)	0.4217(3)	0.0272(12)
N(8)	−0.0666(5)	0.2739(4)	0.3778(3)	0.0260(12)
N(9)	0.0465(4)	0.1987(4)	0.3438(3)	0.0243(10)
H(1)	0.509(7)	0.397(4)	0.448(3)	0.035(18)
H(3)	0.343(6)	0.137(5)	0.324(3)	0.035(18)
H(7)	−0.075(5)	0.411(4)	0.450(3)	0.034(15)
H(8)	−0.152(9)	0.263(8)	0.356(6)	0.141(41)

[a] $U_{eq} = {}^1/_3 \sum_i \sum_j U_{ij} a^*_i a^*_j \mathbf{a}_i \cdot \mathbf{a}_j$.

these water molecules arranged perpendicular to the planes. Two monomeric complex units, which are related by a center of inversion at position 0.5, 0.5, 0.5, are connected to dimers via two relatively strong N(1)–H(1)···O(6) hydrogen-bonding contacts. An interesting structural feature of these compounds is an indirect chelation via an intramolecular hydrogen-bonding contact. This hydrogen-bonding scheme is often observed in conjunction with monodentate coordination of purines. The relatively strong hydrogen bond N(3)–H(3)···O(11), with a donor–acceptor distance of 2.768(1) Å, reveals the formation of a six-membered indirect chelate, whereas the weaker interaction N(3)–H(3)···O(12), with a N···O distance of 3.236(1) Å, results in an eight-membered chelate. In addition, an indirect chelation occurs via the hydrogen-bonding contact N(8)–H(8)···O(11), with a donor–acceptor distance of 3.052(2) Å, forming a five-membered ring system. The interaction N(8)–H(8)···O(13), with a N···O distance of 2.788(1) Å, finally results in the formation of a seven-membered chelate ring.

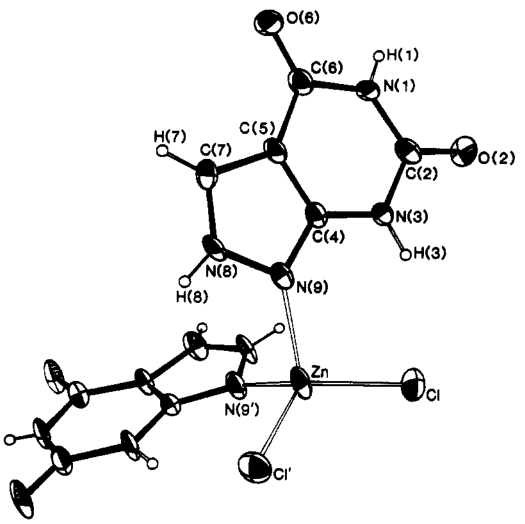

Figure 3. Coordination polyhedron of the zinc atom in Zn(alloxanthine)$_2$Cl$_2$. The thermal ellipsoids shown are drawn at the 50% probability level.

In Zn(alloxanthine)$_2$Cl$_2$, two alloxanthine ligands coordinating to different zinc ions are related by a center of inversion and are connected via two N(1)–H(1)···O(6) hydrogen bonds. The

Table VI. Interatomic Bond Distances (Å) in M(alloxanthine)$_2$(NO$_3$)$_2$·2H$_2$O

	M = Cu	M = Co		M = Cu	M = Co
		Metal Coordination Polyhedron			
M–N(9)	2.038(1) (2×)	2.1833(8) (2×)	M–O(11)	2.353(1) (2×)	2.1401(9) (2×)
M–O(1)	1.962(1) (2×)	2.0224(9) (2×)			
		Alloxanthine			
N(1)–C(2)	1.376(2)	1.385(1)	C(7)–N(8)	1.323(2)	1.328(1)
C(2)–N(3)	1.363(1)	1.369(1)	N(8)–N(9)	1.371(1)	1.371(1)
N(3)–C(4)	1.367(1)	1.367(1)	N(9)–C(4)	1.332(1)	1.336(1)
C(4)–C(5)	1.394(1)	1.403(1)	C(2)–O(2)	1.226(1)	1.218(1)
C(5)–C(6)	1.430(1)	1.431(1)	C(6)–O(6)	1.230(1)	1.236(1)
C(6)–N(1)	1.375(1)	1.374(1)	N(3)–N(9)	2.419(1)	2.421(1)
C(5)–C(7)	1.381(1)	1.388(1)			
		Nitrate			
N(11)–O(11)	1.246(1)	1.262(1)	N(11)–O(13)	1.238(1)	1.240(1)
N(11)–O(12)	1.228(1)	1.235(1)			

Table VII. Interatomic Bond Angles (deg) in M(alloxanthine)$_2$(NO$_3$)$_2$·2H$_2$O

	M = Cu	M = Co		M = Cu	M = Co
		Metal Coordination Polyhedron			
N(9)–M–O(1)	89.58(4)	89.26(4) (2×)	N(9)–M–O(11′)	92.77(4)	92.66(4) (2×)
N(9)–M–O(1′)	90.42(4)	90.74(4) (2×)	O(1)–M–O(11)	89.69(5)	88.54(4) (2×)
N(9)–M–O(11)	87.23(4)	87.34(4) (2×)	O(1)–M–O(11′)	90.31(5)	91.46(4) (2×)
		Alloxanthine			
C(6)–N(1)–C(2)	127.1(1)	127.44(8)	N(8)–N(9)–C(4)	103.7(1)	103.42(7)
N(1)–C(2)–N(3)	117.3(1)	116.82(8)	N(9)–C(4)–C(5)	111.5(1)	111.63(8)
C(2)–N(3)–C(4)	120.4(1)	120.53(8)	N(3)–C(4)–N(9)	127.3(1)	127.14(8)
N(3)–C(4)–C(5)	121.2(1)	121.23(8)	C(6)–C(5)–C(7)	134.1(1)	134.27(9)
C(4)–C(5)–C(6)	120.7(1)	120.58(8)	N(1)–C(2)–O(2)	120.3(1)	120.25(9)
C(5)–C(6)–N(1)	113.3(1)	113.32(8)	N(3)–C(2)–O(2)	122.4(1)	122.92(9)
C(4)–C(5)–C(7)	105.2(1)	105.12(8)	N(1)–C(6)–O(6)	121.0(1)	120.42(9)
C(5)–C(7)–N(8)	106.6(1)	106.17(8)	C(5)–C(6)–O(6)	125.7(1)	126.26(9)
C(7)–N(8)–N(9)	113.1(1)	113.66(8)			
		Metal–Alloxanthine			
M–N(9)–C(4)	137.0(1)	136.04(7)	M–N(9)–N(8)	119.3(1)	120.53(6)
		Nitrate			
O(11)–N(11)–O(12)	119.5(1)	118.7(1)	O(12)–N(11)–O(13)	121.7(1)	121.3(1)
O(11)–N(11)–O(13)	118.8(1)	120.0(1)			

Table VIII. Interatomic Bond Distances (Å) in $Zn(alloxanthine)_2Cl_2$

	Metal Coordination Polyhedron		
Zn–N(9)	2.031(4) (2×)	Zn–Cl	2.204(1) (2×)
	Alloxanthine		
N(1)–C(2)	1.365(6)	C(7)–N(8)	1.319(6)
C(2)–N(3)	1.377(6)	N(8)–N(9)	1.371(5)
N(3)–C(4)	1.383(6)	N(9)–C(4)	1.342(6)
C(4)–C(5)	1.386(7)	C(2)–O(2)	1.221(6)
C(5)–C(6)	1.434(6)	C(6)–O(6)	1.206(6)
C(6)–N(1)	1.394(6)	N(3)–N(9)	2.421(5)
C(5)–C(7)	1.404(7)		

Table IX. Interatomic Bond Angles (deg) in $Zn(alloxanthine)_2Cl_2$

	Metal Coordination Polyhedra		
N(9)–Zn–Cl	104.4(1) (2×)	N(9)–Zn–N(9′)	97.8(2)
N(9)–Zn–Cl′	112.1(9) (2×)	Cl–Zn–Cl′	121.9(1)
	Alloxanthine		
C(6)–N(1)–C(2)	128.9(4)	N(8)–N(9)–C(4)	102.4(4)
N(1)–C(2)–N(3)	116.9(4)	N(9)–C(4)–C(5)	113.0(4)
C(2)–N(3)–C(4)	119.5(5)	N(3)–C(4)–N(9)	125.3(5)
N(3)–C(4)–C(5)	121.7(4)	C(6)–C(5)–C(7)	134.1(5)
C(4)–C(5)–C(6)	121.6(4)	N(1)–C(2)–O(2)	123.1(4)
C(5)–C(6)–N(1)	111.5(5)	N(3)–C(2)–O(2)	120.1(5)
C(4)–C(5)–C(7)	104.1(4)	N(1)–C(6)–O(6)	121.0(4)
C(5)–C(7)–N(8)	106.2(5)	C(5)–C(6)–O(6)	127.5(5)
C(7)–N(8)–N(9)	114.2(4)		
Zn–N(9)–C(4)	131.1(3)	Zn–N(9)–N(8)	124.2(3)

Table X. Hydrogen-Bonding Contacts in $Cu(alloxanthine)_2(NO_3)_2 \cdot 2H_2O$, $Co(alloxanthine)_2(NO_3)_2 \cdot 2H_2O$ in $Zn(alloxanthine)_2Cl_2$

X–H···Y	X–H, Å	H···Y, Å	X–Y, Å	X–H···Y, deg
		$Cu(alloxanthine)_2(NO_3)_2 \cdot 2H_2O$		
N(1)–H(1)···O(6)	0.78(2)	2.05(2)	2.818(1)	173(2)
N(3)–H(3)···O(11)	1.01(2)	1.95(2)	2.768(1)	136(2)
N(3)–H(3)···O(12)	1.01(2)	2.25(2)	3.236(1)	164(2)
N(8)–H(8)···O(11)	0.86(3)	2.48(3)	3.052(2)	125(2)
N(8)–H(8)···O(13)	0.86(3)	1.93(3)	2.788(1)	176(2)
O(1)–H(11)···O(2)	0.90(1)	1.930(1)	2.804(1)	163(1)
O(1)–H(12)···O(6)	0.82(1)	2.212(1)	2.993(2)	161(1)
		$Co(alloxanthin)_2(NO_3)_2 \cdot 2H_2O$		
N(1)–H(1)···O(6)	0.972(1)	1.991(1)	2.878(1)	118.2(1)
N(3)–H(3)···O(11)	0.943(1)	2.184(1)	2.942(1)	136.7(1)
N(3)–H(3)···O(12)	0.943(1)	2.037(1)	2.947(1)	161.8(1)
N(8)–H(8)···O(11)	0.967(1)	2.567(1)	3.157(1)	119.5(1)
N(8)–H(8)···O(13)	0.967(1)	1.824(1)	2.786(1)	172.7(1)
O(1)–H(11)···O(2)	0.886(1)	1.876(1)	2.746(1)	167.2(1)
O(1)–H(12)···O(6)	0.813(1)	2.024(1)	2.803(1)	160.4(1)
		$Zn(alloxanthine)_2Cl_2$		
N(1)–H(1)···O(6)	0.72(5)	2.18(5)	2.903(6)	178(5)
N(3)–H(3)···Cl	0.87(5)	2.43(5)	3.235(5)	153(4)
N(8)–H(8)···O(2)	0.79(8)	2.03(7)	2.747(5)	150(9)

bonding arrangement results in an infinite zigzag chain of the type metal–alloxanthine···alloxanthine–metal. These chains are linked to ribbons parallel to the *a* axis by relatively strong hydrogen-bonding interactions N(8)–H(8)···O(2), with donor–acceptor distances of 2.747(5) Å. A weak intramolecular hydrogen bond N(3)–H(3)···Cl, with a N···Cl distance of 3.235(5) Å, again reveals the formation of an indirect six-membered chelate ring, since the alloxanthine molecule and the chloride ion are coordinated to the same zinc ion.

A packing diagram of the complexes $M(alloxanthine)_2(NO_3) \cdot 2H_2O$ is presented in Figure 4. The alloxanthine ligands are infinitely stacked along the *a* axis of the unit cell with only minor direct overlap of the pyrazole rings. The mean stacking distance is 3.33 Å. In addition, the nitrate groups are stacked along the *a* axis of the unit cell on top of the six-membered rings of the alloxanthine ligands. The packing diagram of the complex $Zn(alloxanthine)_2Cl_2$ is illustrated in Figure 5. There is no infinite stacking of alloxanthine molecules in this complex, but nearly parallel (dihedral angle 3°) planes of two molecules at a time are stacked with a mean spacing distance of 3.25 Å.

In all complexes presented here, the coordinating alloxanthine ligands show a slight nonplanarity in the pseudoaromatic ring system. Maximum deviations of an individual ring atom from the least-squares plane through the nine ring atoms are 0.02 Å (Cu), 0.03 Å (Co) and 0.04 Å (Zn).

Coordinating Properties of Alloxanthine. The compounds described in this paper represent the first structurally characterized metal complexes of alloxanthine. In all three compounds, the neutral 1H,3H,8H-tautomer of alloxanthine is monodentately coordinating to the metal center through its unprotonated pyrazole nitrogen atom N(9). This complexation behavior of alloxanthine can be compared with that of other neutral oxopurines and their derivatives, as follows:

Neutral *allopurinol*, the biological precursor of alloxanthine, exhibits two different coordination types. In monomeric complexes,[15-17] metalation predominantly occurs through the pyrazole nitrogen atom N(8). N(9)-coordination could only be observed in one organometallic rhodium complex.[18] The preferred coordination through the sterically less restricted site N(8) might explain the high affinity of allopurinol for the molybdenum center of xanthine oxidase.

Crystallographic investigations on metal complexes containing neutral *xanthine* have revealed structural analogies, including N(9)-coordination with the alloxanthine complexes described in this paper. The structure analysis of $Cu(xanthine)_2(NO_3)_2 \cdot 2H_2O$[19] has established an isostructural relationship with the complexes of the type $M(alloxanthine)_2(NO_3)_2 \cdot 2H_2O$ with M = Cu and Co. In addition, a structure closely related to that of $Zn(alloxanthine)_2Cl_2$ has been confirmed for the complex $Zn(xanthine)_2Cl_2$.[19] Obviously, neutral xanthine and its 7-deaza-8-aza-derivative alloxanthine are predominantly coordinating through the imidazole nitrogen atom N(9).

In *hypoxanthine* complexes, the imidazole nitrogen atom N(7) has been established as the preferred coordination site in monomeric structures.[20-22] Bridging of two metal ions by N(3)/N(9)-chelating hypoxanthine ligands seems to be the predominant structure type for dimeric complexes.[23-25] Finally, in a polymeric structure of a copper complex, hypoxanthine coordinates through N(3) and N(7) to different metal ions, forming infinite copper hypoxanthine chains.[20]

Quantum Chemical Calculations. We have tried to rationalize the observed tendency of alloxanthine to coordinate through its nitrogen atom N(9) by quantum chemical calculations at the semiempirical and the ab initio levels using the MIDI basis set. The molecular electrostatic potential has been calculated for the optimized geometries, and the probability of metal coordination at different sites can be discussed in terms of contour diagrams of this potential in the molecular plane. For alloxanthine, the contour diagram (Figure 6) of the 1H,3H,8H-tautomer clearly documents the attractivity of the position N(9) for metal ions. Ab initio calculations predict that this tautomer is more stable than the 1H,3H,9H-tautomer by about 13 kJ·mol^{-1}.[26]

---

(15) Hänggi, G.; Schmalle, H.; Dubler, E. *Acta Crystallogr., Sect. C: Cryst. Struct. Commun.* **1991**, *C47*, 1609.
(16) Hänggi, G.; Schmalle, H.; Dubler, E. *Inorg. Chem.* **1988**, *27*, 3131.
(17) Hänggi, G.; Schmalle, H.; Dubler, E. *Acta Crystallogr., Sect. C: Cryst. Struct. Commun.* **1988**, *C44*, 1560.
(18) Sheldrick, W. S.; Günther, B. *Inorg. Chim. Acta* **1988**, *151*, 237.
(19) Dubler, E.; Hänggi, G.; Schmalle, H. *Inorg. Chem.* **1992**, *31*, 3728.
(20) Dubler, E.; Hänggi, G.; Bensch, W. *J. Inorg. Biochem.* **1987**, *29*, 269.
(21) Dubler, E.; Hänggi, G.; Schmalle, H. *Acta Crystallogr., Sect. C: Cryst. Struct. Commun.* **1987**, *C43*, 1872.
(22) Kastner, M. E.; Coffey, K. F.; Clark, M. J.; Edmonds, S. E.; Eriks, K. *J. Am. Chem. Soc.* **1981**, *103*, 5747.
(23) Dubler, E.; Hänggi, G.; Schmalle, H. *Inorg. Chem.* **1990**, *29*, 13, 2518.
(24) Hänggi, G.; Schmalle, H.; Dubler, E. *Acta Crystallogr., Sect. C: Cryst. Struct. Commun.* **1992**, *C48*, 1008.
(25) Sletten, E. *Acta Crystallogr., Sect. B: Struct. Crystallogr. Cryst. Chem.* **1970**, *B26*, 1609.
(26) Nonella, M.; Hänggi, G.; Dubler, E. *THEOCHEM* **1993**, *279*, 173.

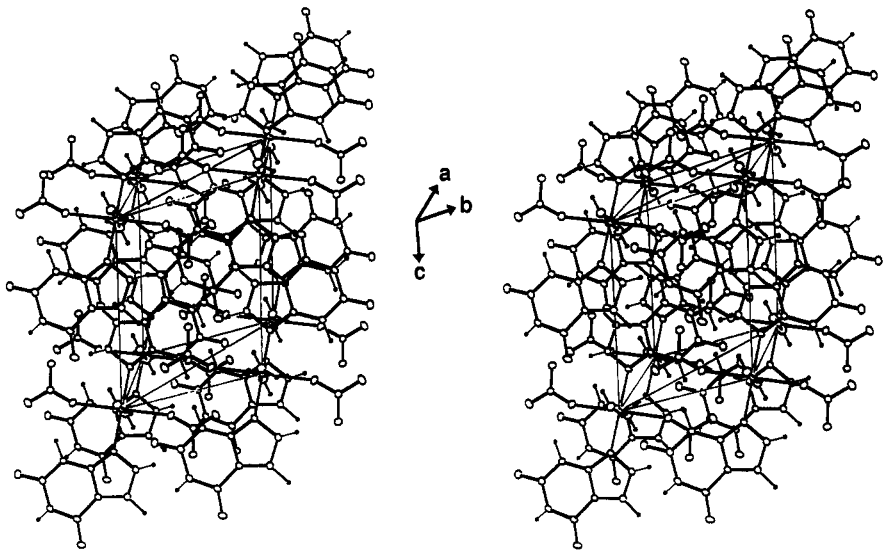

Figure 4. Stereoview of the unit cell of M(alloxanthine)$_2$(NO$_3$)$_2$·2H$_2$O (M = Cu, Co). The parameters drawn refer to the copper complex.

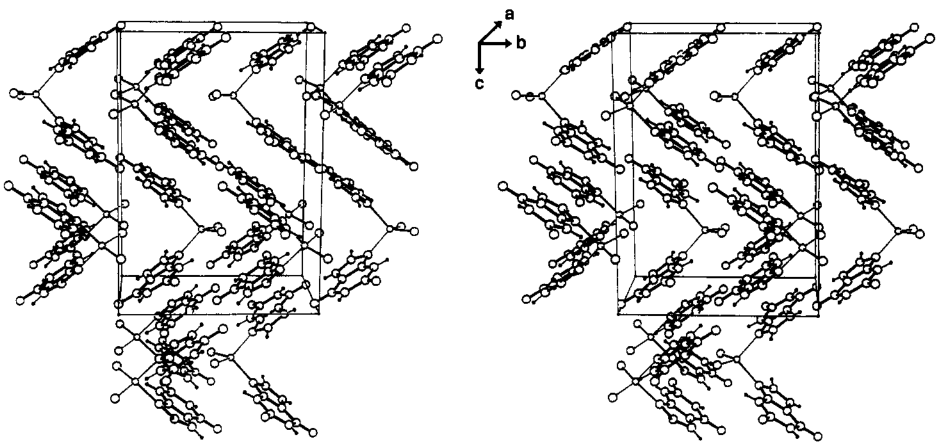

Figure 5. Stereoview of the unit cell of Zn(alloxanthine)$_2$Cl$_2$.

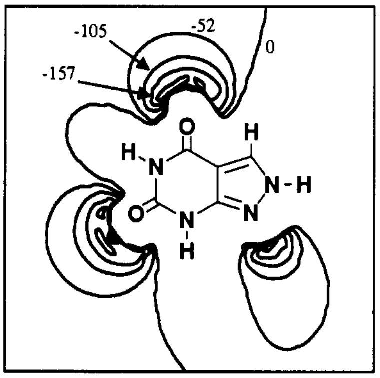

Figure 6. Negative (attractive) part of the electrostatic potential (kJ·mol^{-1}) within the molecular plane of the 1H,3H,8H-tautomer of alloxanthine, calculated with the MIDI basis set.

Biochemical Aspects. Alloxanthine forms a tight complex with the reduced state of the molybdenum center of xanthine oxidase, thus effectively inhibiting the action of the enzyme. In contrast, allopurinol seems to have a pronounced affinity for coordination to molybdenum in the oxidation state VI.[8] The different coordinating properties of these two purine derivatives presumably are an important factor determining the mechanism of inhibition within the catalytic cycle.

Considerable efforts have been directed toward elucidating the structure of the molybdenum center of xanthine oxidase being bound by an inhibitory molecule. A recent review of this subject is given by Holm.[27] EXAFS investigations by Hille[8] and Turner[28] show that the coordination of the reduced molybdenum(IV) form (the relevant oxidation state with respect to the enzyme alloxanthine complex) includes two or three thiolate-like sulfurs, probably relating to the molybdenum cofactor, and one single oxo group. The oxidized form, in contrast, also shows M═S coordination.[8,27] In addition, EPR signals obtained on partial oxidation of the enzyme inhibitor complex show resolved ^{14}N hyperfine coupling that may originate from a coordinating nitrogen atom.[9] According to these data, a structural model in

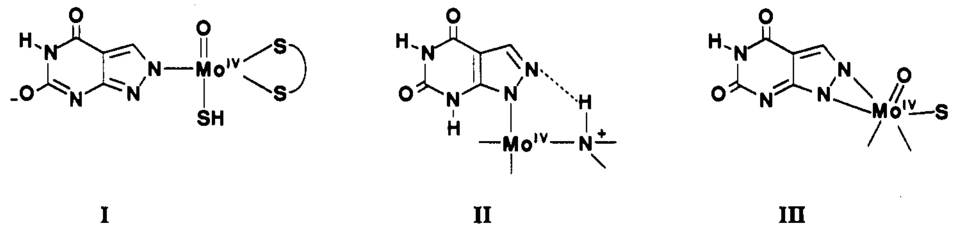

Figure 7. Different structure types proposed for the molybdenum alloxanthine inhibitory complex in xanthine oxidase: (I) coordination through N(8) (Hille,[8] Hawkes[9]); (II) coordination through N(9) (Stiefel[29]); (III) bidentate coordination through N(8)/N(9) (Robins[30]).

which alloxanthine coordinates to the molybdenum through one of the four ring nitrogen atoms was proposed. With regard to the origin of the coupled nitrogen atom, Hawkes[9] has proposed a metal-binding pattern where alloxanthine is ligated via the pyrazole nitrogen atom N(8) to molybdenum (Figure 7, structure type I). This model is also strongly supported by the work of Hille.[8] Stiefel,[29] however, suggests an inhibitor complex with alloxanthine monodentately coordinating through the pyrazole nitrogen atom N(9), stabilized by a strong N(8)–H(8)···N(enzyme) hydrogen bond (Figure 7, structure type II). In a third model, the high stability of the enzyme inhibitor complex has even been explained by an unusual bidentate coordination of alloxanthine through both pyrazole nitrogen atoms N(8) and N(9) (Figure 7, structure type III).[30]

The experimental data presented in this paper support those models of the inhibition of xanthine oxidase by alloxanthine which assume metal coordination through N(9) of alloxanthine.

Acknowledgment. Research grants from the Swiss National Science Foundation (No. 21-27924.89) are gratefully acknowledged.

Supplementary Material Available: Tables of anisotropic thermal parameters and bond distances and angles involving hydrogen atoms (4 pages). Ordering information is given on any current masthead page. Lists of structure factors may be obtained from the authors.

---

(27) Holm, R. H. *Coord. Chem. Rev.* **1990**, *100*, 183.

(28) Turner, N. A.; Bray, R. C.; Diakun, G. P. *Biochem. J.* **1989**, *260*, 563.

(29) Stiefel, E. I. *Prog. Inorg. Chem.* **1977**, *22*, 1.

(30) Robins, K.; Revankar, G. R.; O'Brien, D. E.; Springer, R. H.; Novinson, T.; Albert, A.; Senga, K.; Miller, J. P.; Streeter, D. G. *J. Heterocycl. Chem.* **1985**, *22*, 601 and references therein.